Modellization and Control of Spurious Frequency Generation due to Rayleigh Backscattering in Low-Frequency-Radio over Fiber Systems for Radioastronomic Application

Andrea Giovannini (1), Jacopo Nanni (1), Simone Rusticelli(2),
Randall Wayth(3), Enrico Lenzi (4), Federico Perini(2), Jader Monari(2), Giovanni Tartarini(1)

[1]*DEI - University of Bologna, Bologna, viale del Risorgimento 2, Italy*
[2] *IRA-INAF, Medicina (Bologna), Via Fiorentina 3513, Italy*
[3] *Curtin University, Bentley Western Australia, 6102*
[4] *Protech S.a.S, Castelfranco Veneto (TV), Via dei Pini 21, Italy*

Presentation overview

- Symbols definition and references ……………………………………………… 3
- SKA and contextualization of the work ………………………………………. 5
- Developed model ………………………………………………………………………. 9
- Experimental results ……………………………………………………………… 19
- Conclusions …………………………………………………………………………………. 24

Symbols definition and references

Symbol	Description	Slide #
m	Intensity modulation index	9, 10
ω_{RF}	Modulating tone angular frequency	9, 10, 16, 18
ω_0	Carrier angular frequency	9, 10
a_2	Laser's second order non-linearity index	9, 10
a_3	Laser's third order non-linearity index	9, 10
τ_z	Time required to travel a distance z into the fiber	9, 10, 12, 15, 16, 18, 21
β	Fiber's propagation coefficient	9, 10
α	Fiber's attenuation coefficient	9, 10

Symbols definition and references

Symbol	Description	Slide #
M	Laser chirp coefficient	9, 10, 16, 18, 21
$\varphi(t)$	Phase noise	9, 10
$\rho(z)$	Rayleigh backscattering reflection coefficients	11, 12, 14, 16
σ^2	Variance of $\rho(z)$	14
$\mathcal{R}$	Photodetector responsivity	13
L	Length of the fiber	12, 13, 15, 16
$\Delta\omega$	Laser linewidth	15, 16, 17, 18
v_{g}	Group velocity	15, 16

SKA and contextualization of the work

- **Square Kilometre Array (SKA) concept**
  - Largest Radio-Telescope composed of 130.000 antennas connected to a central processing station
  - SKA-LOW (Australia) [50-350] MHz
  - SKA-MID (South Africa) [0.35-14] GHz
  - Several kilometers of distance between each antenna and the central processing unit
    → Radio-over-Fiber (RoF)

- **Aperture Array Verification Systems (AAVS) for SKA-LOW**
  - Verification system of 256 Antennas developed in Australia
  - To verify the performances of the RoF links in terms of stability, linearity, etc…

SKA and contextualization of the work

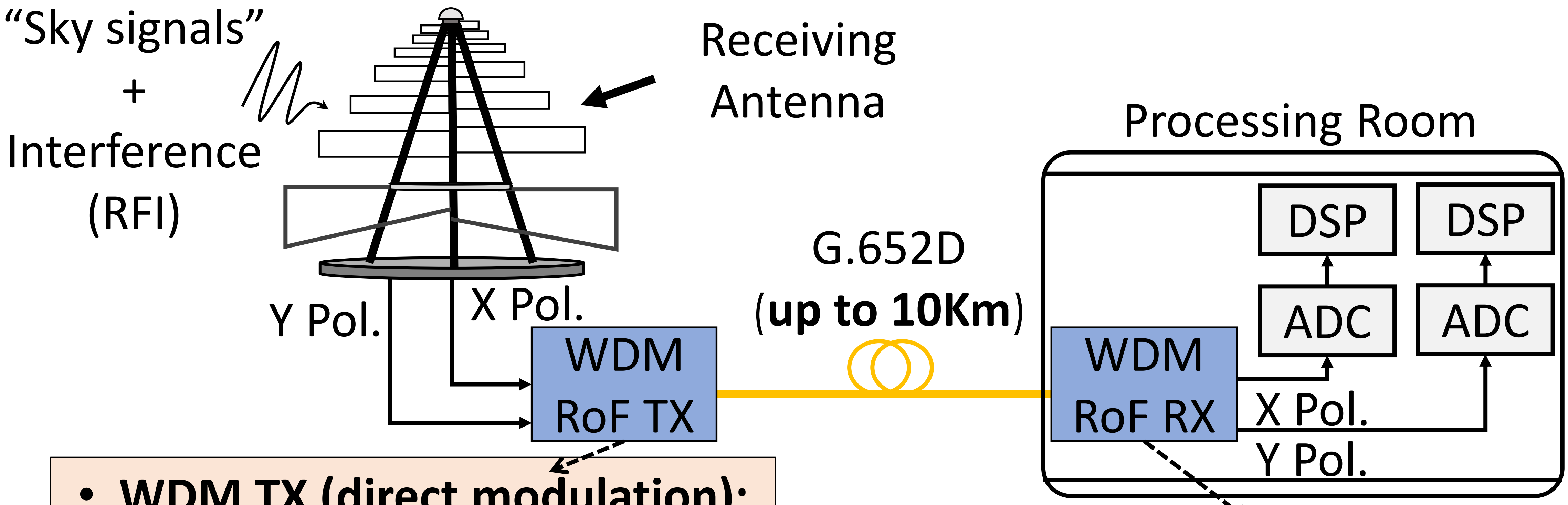

- **WDM TX (direct modulation):**

  $\lambda_X = 1270\text{ nm}, P_X = 4dBm$

  $\lambda_Y = 1330\text{ nm}, P_Y = 4dBm$

- **WDM RX (direct detection)**
- **Post-Amp**

<u>Study of the nonlinearities of the pure optical system in presence of RFI</u>

SKA and contextualization of the work

- Study on single polarization channel (1330nm)
- RFI at 70 MHz as example (sinusoidal tone) injected into the system
- Carrier (C)-to-2nd Harmonic Distortion (HD2) ratio vs RF laser input power ($P_{RF,IN}$)

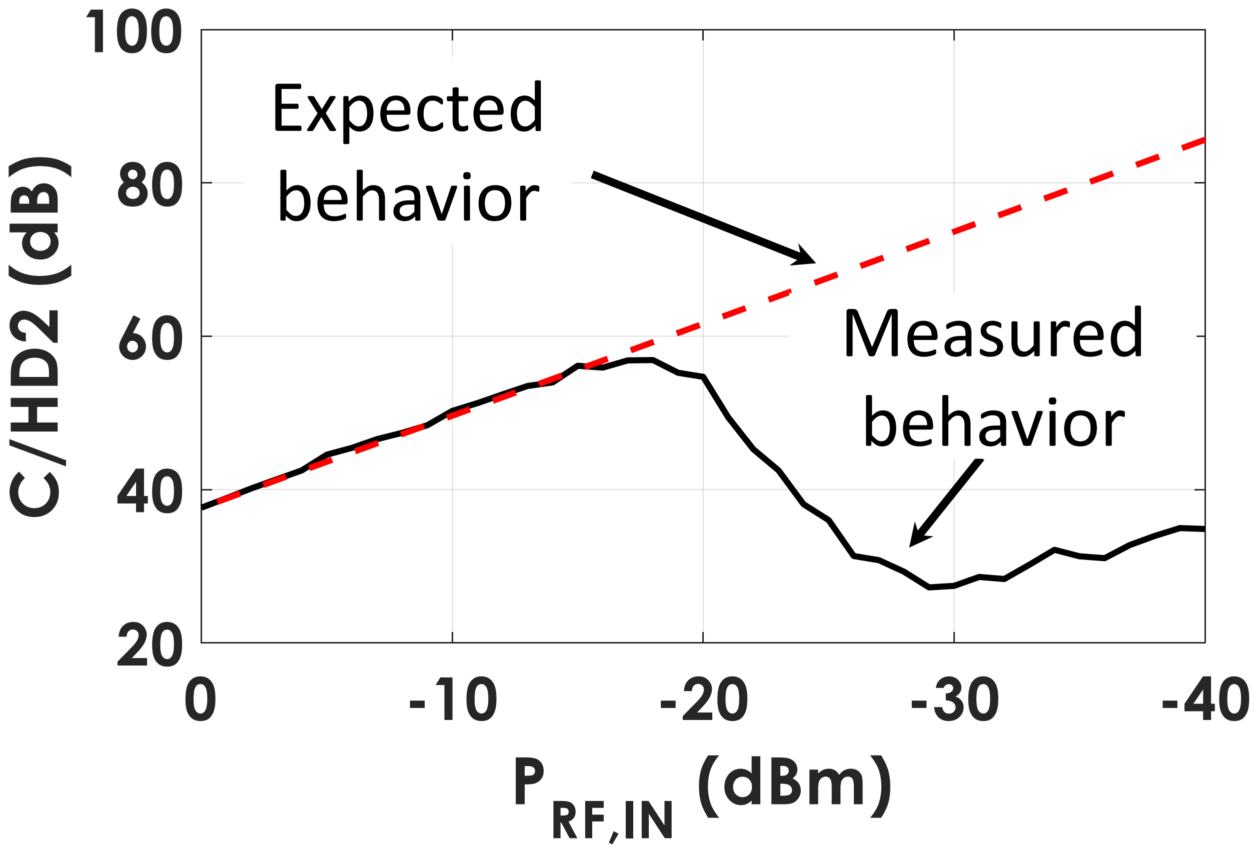

High HD2 for $P_{RF,IN} \in [-60, -24] dBm$ → Cause: **Rayleigh Backscattering**

SKA and contextualization of the work

- Study on single polarization channel (1330nm)
- 2 RFI tones at 70MHz and 72MHz as example (sinusoidal tone) injected into the system
- Carrier (C)-to-2nd Intermodulation Distortion (IMD2) ratio vs RF laser input power ($P_{RF,IN}$)

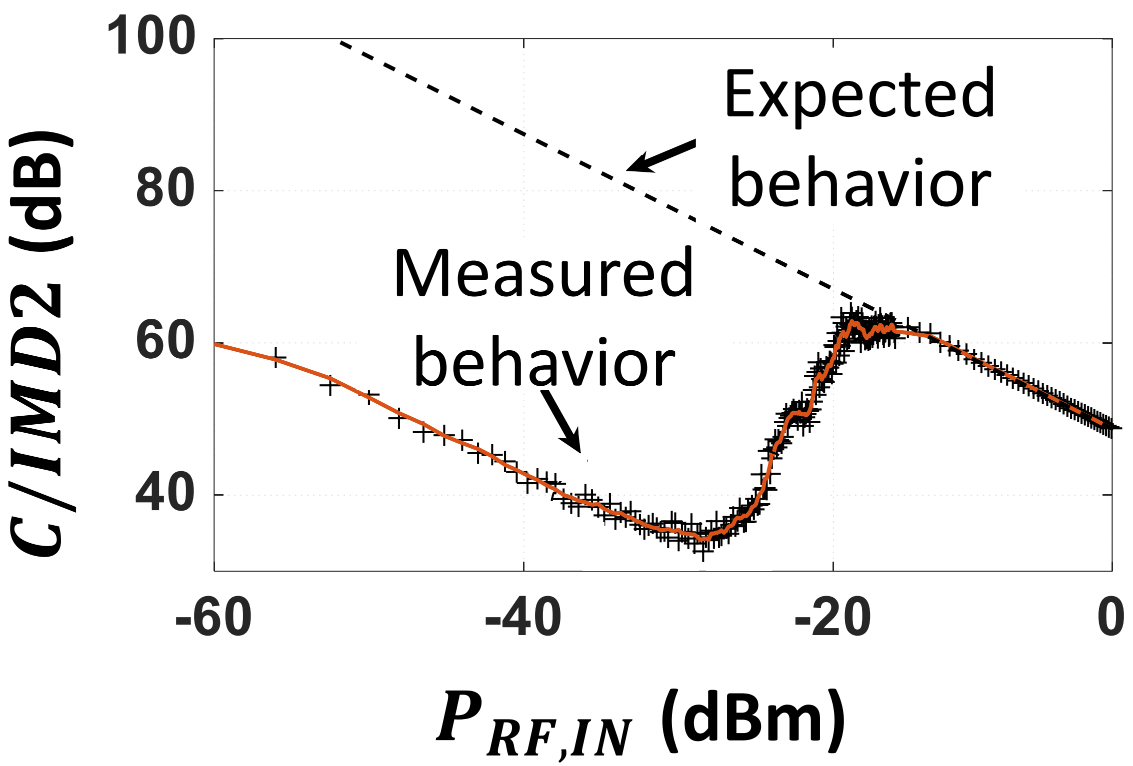

High IMD2 for $P_{RF,IN} \in [-60,-24]dBm$ → Cause: **Rayleigh Backscattering**

Developed model

Consider a RoF link with a laser modulated by a single RF tone. The propagating field is given by the expression:

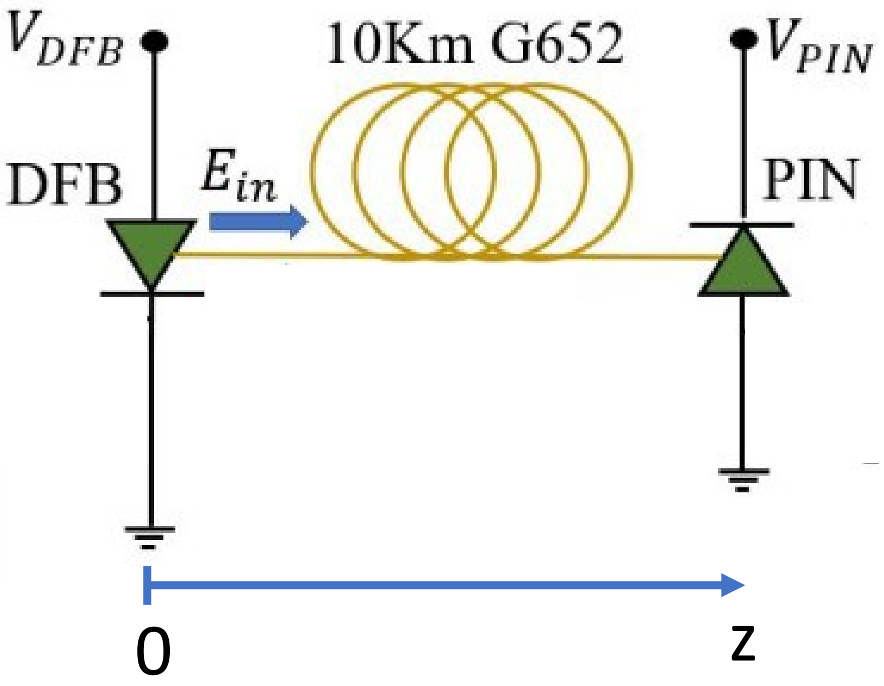

$$E_{in}(t,z) = E_0\{1 + [m\,cos(\omega_{RF}(t-\tau_z))] +$$

$$+ a_2[\ldots]^2 + a_3[\ldots]^3\}^{1/2} e^{-j\beta z} e^{-\frac{\alpha}{2}z} \cdot$$

$$\cdot\, e^{jM sin(\omega_{RF}(t-\tau_z))} e^{j\varphi(t-\tau_z)} e^{-j\omega_0(t-\tau_z)}$$

NB: $[\ldots]$ stands for $[m\,cos(\omega_{RF}(t-\tau_z))]$

Developed model

The expression of $E_{in}(t,z)$ accounts for:

- Laser modulation. (___)
- Laser non-linearities. (___)
- Laser chirp. (___)
- Phase noise. (___)

$$E_{in}(t,z) = E_0\{1 + [m\,cos(\omega_{RF}(t-\tau_z))] + a_2[\dots]^2 + a_3[\dots]^3\}^{1/2} e^{-j\beta z} e^{-\frac{\alpha}{2}z} \cdot e^{jMsin(\omega_{RF}(t-\tau_z))} e^{j\varphi(t-\tau_z)} e^{-j\omega_0(t-\tau_z)}$$

Developed model

An infinitesimal section of the fiber scatters a portion ρ of the propagating field backwards, due to Rayleigh bacscattering. Summing all these small contributions gives the total backscattered field.

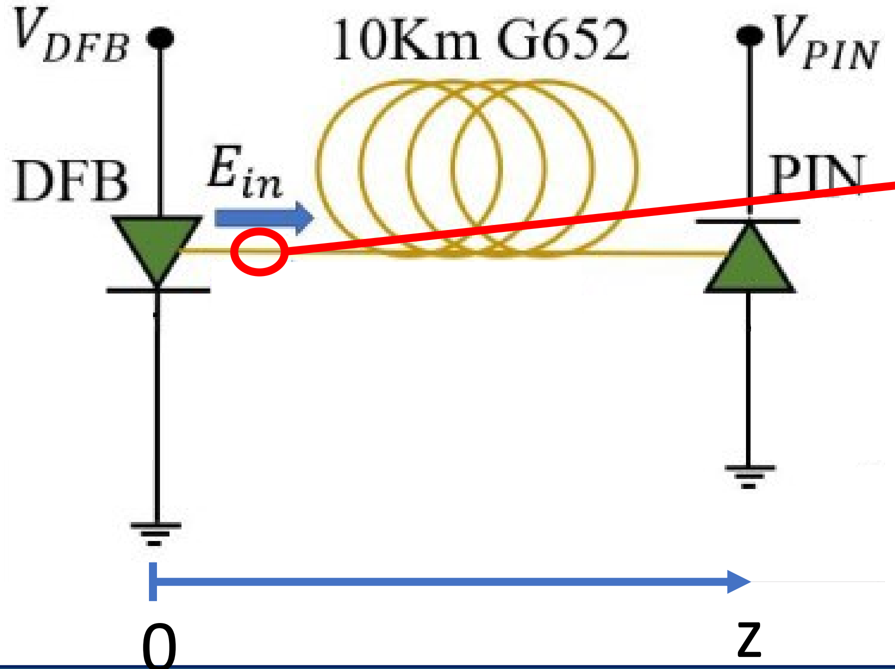

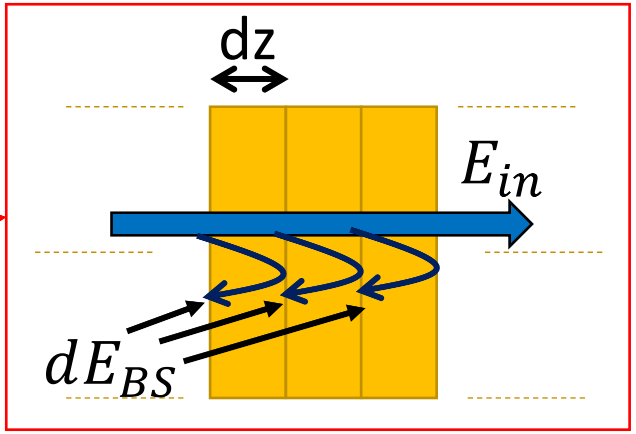

Infinitesimal sections of the fiber

$$dE_{BS}(t,z) = \rho(z)E_{in}(t,z)$$

$\rho(z)$ are delta correlated zero-mean circular complex Gaussian random variables.

Developed model

The total backscattered field at section z = 0 is then:

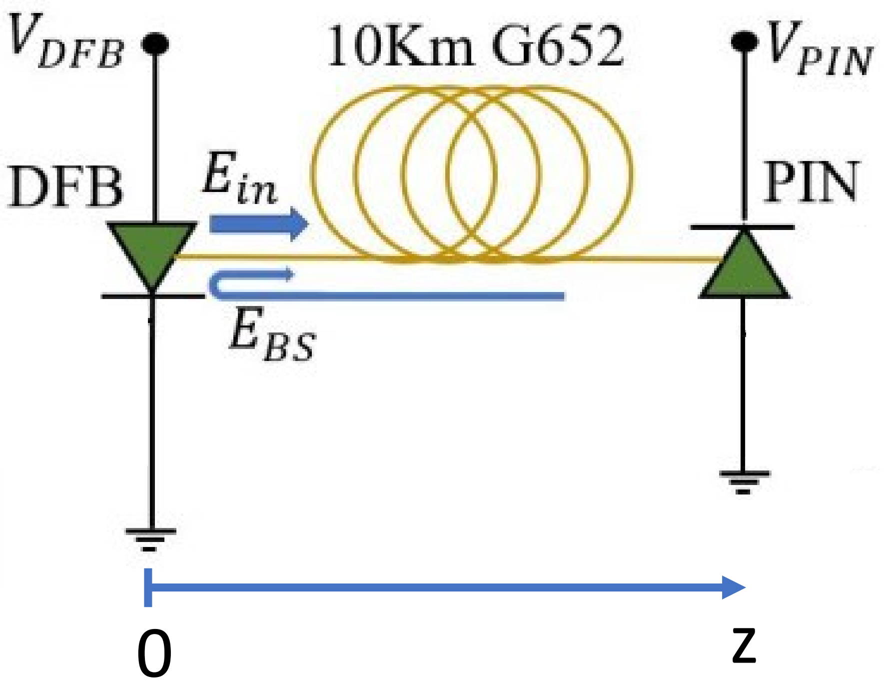

$$E_{BS}(t, z = 0) = \int_0^L E_{in}(t - 2\tau_z, z)\rho(z)dz$$

While at section z = L it becomes:

$$E_{BS}(t, z = L) = \int_0^L E_{in}(t - 2\tau_z - \tau_L, z)\rho(z)dz$$

Developed model

The total field at receiver side is the sum of the propagating and of the backscattered fields:

$$E(t,L) = E_{in}(t,L) + E_{BS}(t,L)$$

The detected current is then:

$$i_{out}(t) = \mathcal{R}\,|E(t,L)|^2 \approx \mathcal{R}|E_{in}(t,L)|^2 + 2\Re\mathrm{e}\{\mathcal{R}E_{in}(t,L)E_{BS}^{*}(t,L)\} = i_s(t) + i_{s,BS}(t)$$

NB: $\mathcal{R}|E_{BS}(t,L)|^2$ is negligible compared to the other terms.

Developed model

For the spectral properties of the received current i_{out}, the autocorrelation is firstly evaluated:

$$i_{out}(t) = i_s(t) + i_{s,BS}(t)$$

$$\downarrow \qquad \downarrow \qquad \downarrow$$

$$R_{out}(\xi) = R_s(\xi) + R_{s,BS}(\xi)$$

$$R_x(\xi) = \lim_{T\to\infty} \frac{1}{T} \int_{-\frac{T}{2}}^{\frac{T}{2}} \langle i_x(t)[i_x(t-\xi)]^* \rangle dt$$

This is true due to the definition of the backscattering coefficients $\rho(z)$, which have the property:

$$\langle \rho(z_1)\rho^*(z_2) \rangle = 2\sigma^2\, \delta(z_1 - z_2)$$

NB: $\langle\cdot\rangle$ denotes the the ensemble average. 'x' is either 'out', 'S' or 'S,BS'.

Developed model

While the derivation of $R_s(\xi)$ is more straightforward, to obtain $R_{s,BS}(\xi)$ some lengthy calculation is required. In both cases, we assume the modulation index m to be negligibly small.

$$R_{s,BS}(\xi) \approx \sum_{p=-\infty}^{+\infty} \left(A_p + B_p e^{-\Delta\omega|\xi|}\right) cos(p\omega\xi)$$

$$A_p = 2|E_0|^4 \int_0^{\frac{v_g|\xi|}{2}} g_p(z) e^{-2\Delta\omega\tau_z} dz$$

$$B_p = 2|E_0|^4 \int_{\frac{v_g|\xi|}{2}}^{L} g_p(z) dz$$

Developed model

A_p and B_p condense the effects of both phase noise and laser chirp. The most important terms are the first kind Bessel functions ${J_p}^2\left(2M\,sin\left(\omega_{RF}\frac{\tau_z}{2}\right)\right)$, inside $g_p(z)$. A_p and B_p are in fact averages over z of these Bessel terms weighted by z-dependent coefficients.

$$A_p = 2|E_0|^4 \int_0^{\frac{v_g|\xi|}{2}} g_p(z)e^{-2\Delta\omega\tau_z}dz$$

$$B_p = 2|E_0|^4 \int_{\frac{v_g|\xi|}{2}}^{L} g_p(z)dz$$

$$g_p(z) = |\rho(z)|^2{J_p}^2\left(2M\,sin\left(\omega_{RF}\frac{\tau_z}{2}\right)\right)e^{-2\alpha z}$$

Developed model

The power spectrum of the backscattered field is then:

$$S_{s,BS}(f) = \mathcal{F}\{R_{s,BS}(\xi)\} = \sum_{p=-\infty}^{+\infty} \left[A_p \delta(f - pf_{RF}) + 2B_p \frac{\Delta\omega}{\Delta\omega^2 + \big(2\pi(f - pf_{RF})\big)^2} \right]$$

Which is a series of Dirac deltas and Lorentzian shaped curves centered in integer multiples of the modulating tone frequency.

Developed model

If the laser is modulated by two tones f_{RF1} and f_{RF2} the spectrum becomes:

$$S_{s,BS}(f) = \sum_{p=-\infty}^{+\infty} \sum_{q=-\infty}^{+\infty} \left[A_{p,q}\delta(f - pf_{RF1} - qf_{RF2}) + \frac{2B_{p,q}\Delta\omega}{\Delta\omega^2 + \left(2\pi(f - pf_{RF1} - qf_{RF2})\right)^2} \right]$$

With $A_{p,q}$ and $B_{p,q}$ related to the product $J_p{}^2\left(2M_1\, sin\left(\omega_{RF1}\frac{\tau_z}{2}\right)\right)$ $J_q{}^2\left(2M_2\, sin\left(\omega_{RF2}\frac{\tau_z}{2}\right)\right)$. This case can be extended to more than two tones.

Experimental results

About the setup:

- A signal generator outputs 2 RF tones which modulates a DFB laser.
- The laser feeds a 10 km long G652 standard single mode fiber.
- A PIN photodetector receives both the direct and backscattered fields.
- A low noise amplifier and a signal analyzer post-process the received current.

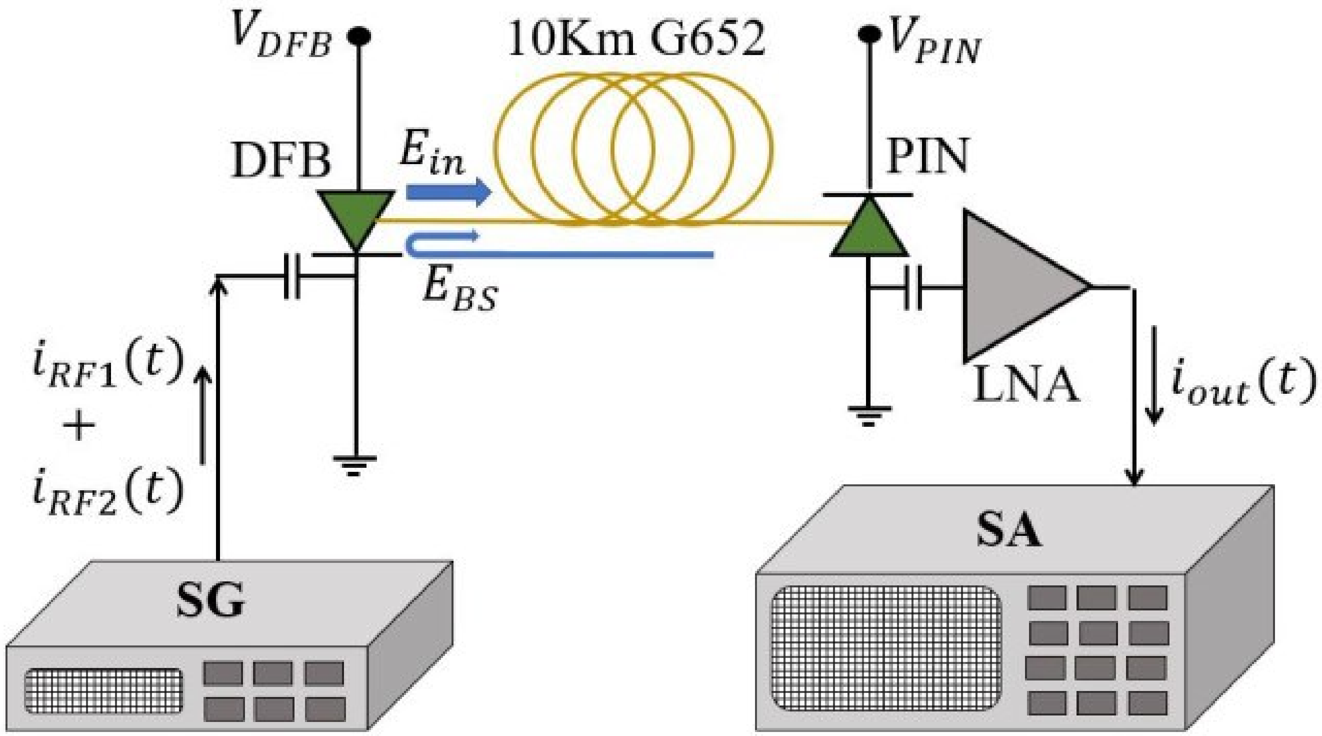

Experimental results

Firstly, in order to prove the model previously descripted, two tones at frequencies of 60 MHz and 75 MHz are generated.

By monitoring HD2 of the first frequency as an example (i.e. 120 MHz), it can be noted that the model suits well with the measurements. Thus proving the effectiveness of the model.

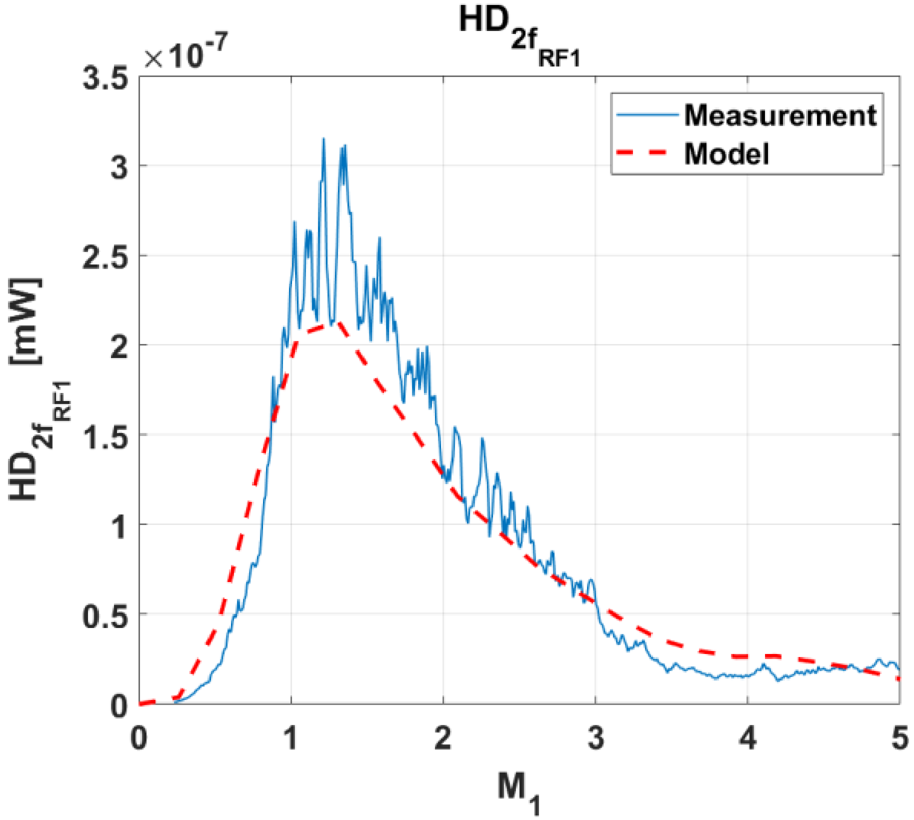

Experimental results

Secondly, a countermeasure to Rayleigh backscattering, called dithering, is proved experimentally. In this case, the first tone is set at 70 MHz, while the second one at a much lower frequency, 10 kHz, which ’dithers’ the laser.

- Dithering repress the backscattering effect because the chirping coefficient related to the dithering frequency is much higher than the other. In particular, the term $J_q{}^2\left(2M_{dith}\,sin\left(\omega_{dith}\frac{\tau_z}{2}\right)\right)$ is responsible for this mitigation.
- Inevitably, applying dithering generates spurious intermodulation terms, which need to be kept at bay.

Experimental results

This figure shows the behavior of HD2 relative to 70 MHz (i.e. 140 MHz) at the variation of the chirping coefficients of the two tones.

For a fixed value of M_1, HD2 lowers if M_{dith} grows, i.e. if the dithering current increases.

NB: Yellow corresponds to higher values, while green and blue to lower ones.

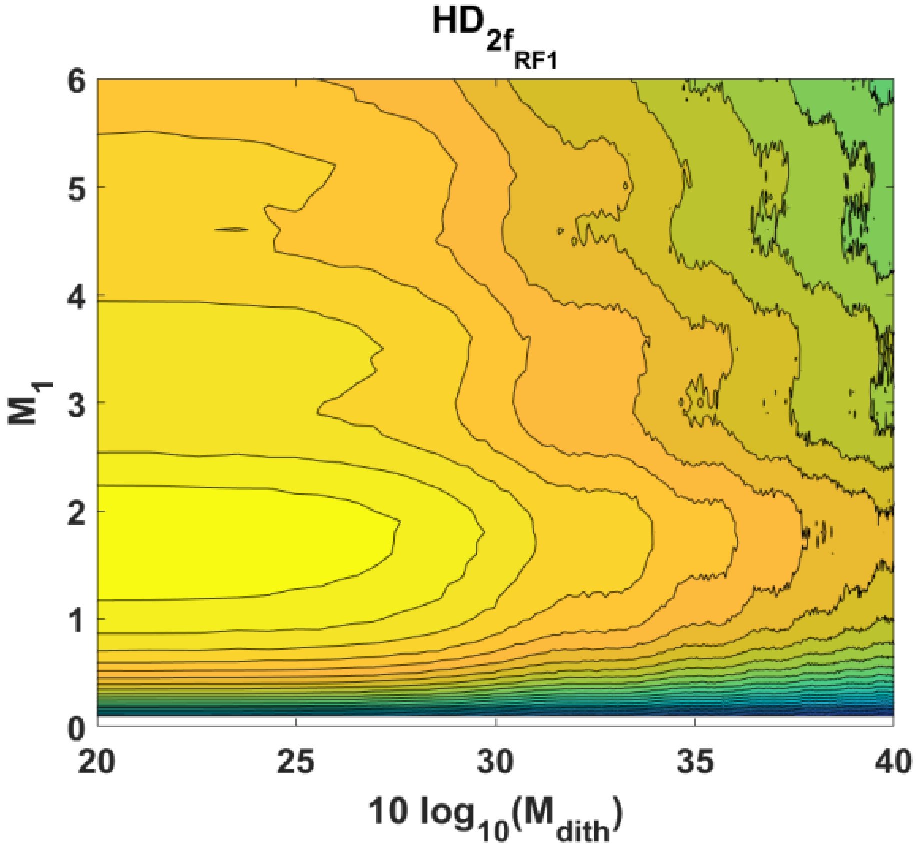

Experimental results

This figure shows the behavior of IMD2 (i.e. 70 MHz + 10 kHz) at the variation of the chirping coefficients of the two tones.

In this case, for a fixed value of M_1, IMD2 initially grows to a maximum peak and only then starts lowering.

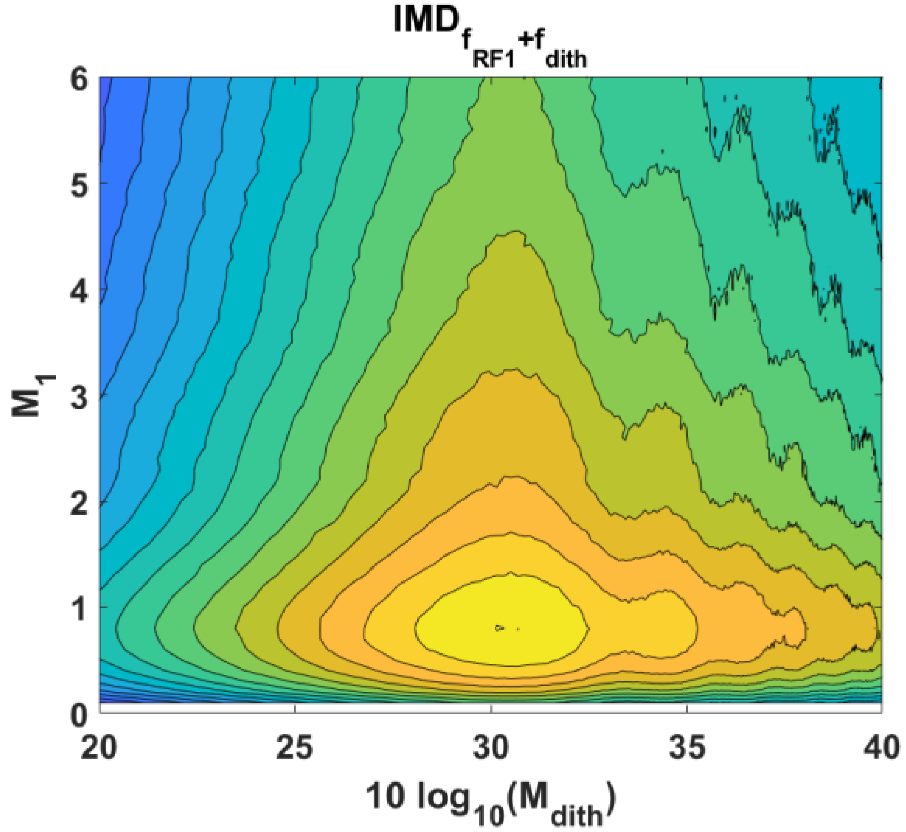

NB: Yellow corresponds to higher values, while green and blue to lower ones.

Conclusions

- A rigorous theoretical model which allows the study of undesired Rayleigh Backscattering-induced nonlinearities in Radio over Fiber Links has been presented and successfully validated.

- A solution to these nonlinearities, namely the introduction of a dithering tone, has been experimentally proven and the developed model allowed to identify the optimal range of values of dithering current amplitudes.